

# Linear Optical, Quadratic and Cubic Nonlinear Optical, Electrochemical, and Theoretical Studies of “Rigid-Rod” Bis(Alkynyl)Ruthenium Complexes<sup>\*\*</sup>,†

Bandar A. Babgi,<sup>[a,b]</sup> Mahesh S. Kodikara,<sup>[a,c]</sup> Mahbod Morshedi,<sup>[a]</sup> Huan Wang,<sup>[a,d]</sup> Cristóbal Quintana,<sup>[a]</sup> Torsten Schwich,<sup>[a]</sup> Graeme J. Moxey,<sup>[a]</sup> Nick Van Steerteghem,<sup>[e]</sup> Koen Clays,<sup>[e]</sup> Robert Stranger,<sup>[a]</sup> Marie P. Cifuentes,<sup>[a]</sup> and Mark G. Humphrey<sup>\*[a]</sup>

**Abstract:** The syntheses of oligo(*p*-phenyleneethynylene)s (OPEs) end-functionalized by a nitro acceptor group and with a ligated ruthenium unit at varying locations in the OPE chain, namely *trans*-[Ru{(C≡C-1,4-C<sub>6</sub>H<sub>4</sub>)<sub>n</sub>NO<sub>2</sub>)(C≡CR)(dppe)<sub>2</sub>] (dppe = 1,2-bis(diphenylphosphino)ethane; n = 1, R = 1,4-C<sub>6</sub>H<sub>4</sub>C≡C-1,4-C<sub>6</sub>H<sub>4</sub>C≡CPh, 1,4-C<sub>6</sub>H<sub>4</sub>NEt<sub>2</sub>; n = 2, R = Ph, 1,4-C<sub>6</sub>H<sub>4</sub>C≡CPh, 1,4-C<sub>6</sub>H<sub>4</sub>C≡C-1,4-C<sub>6</sub>H<sub>4</sub>C≡CPh, 1,4-C<sub>6</sub>H<sub>4</sub>NO<sub>2</sub>, 1,4-C<sub>6</sub>H<sub>4</sub>NEt<sub>2</sub>; n = 3, R = Ph, 1,4-C<sub>6</sub>H<sub>4</sub>C≡CPh), are reported. Their electrochemical properties were assessed by cyclic voltammetry, their linear optical properties and quadratic and cubic nonlinear optical properties assayed by UV/Vis/NIR spectroscopy, hyper-Rayleigh scattering studies employing ns pulses at 1064 nm, and broad spectral range Z-scan studies employing fs pulses, respectively, and their linear optical

properties and vibrational spectroscopic behaviour in the formally Ru<sup>III</sup> state examined by UV/Vis/NIR and IR spectroelectrochemistry, respectively. The potentials of the metal-localized oxidation processes are sensitive to alkynyl ligand modification, but this effect is attenuated on  $\pi$ -bridge lengthening. Computational studies employing time-dependent density functional theory were undertaken on model complexes, a 2D scan revealing a soft potential energy surface for intra-alkynyl-ligand aryl ring rotation, consistent with the experimentally observed blue-shift in optical absorption maxima. Quadratic optical nonlinearities are significant and cubic NLO coefficients for these small complexes are small; the optimum length of the alkynyl ligands and the ideal metal location in the OPE to maximize the key coefficients have been defined.

[a] Dr B. A. Babgi, M. S. Kodikara, Dr M. Morshedi, H. Wang, C. Quintana, Dr T. Schwich, Dr G. J. Moxey, Em. Prof. R. Stranger, Assoc. Prof. M. P. Cifuentes, Prof. M. G. Humphrey  
Research School of Chemistry, Australian National University, Canberra, ACT 2601, Australia  
E-mail: mark.humphrey@anu.edu.au

[b] Current position: Assoc. Prof. B. A. Babgi  
Department of Chemistry, Faculty of Science,  
King Abdulaziz University, Jeddah 21589, Saudi Arabia

[c] Current position: M. S. Kodikara  
Department of Chemistry, University of Ruhuna, Matara 81000,  
Sri Lanka

[d] H. Wang  
School of Chemical and Material Engineering, Jiangnan University,  
Wuxi, Jiangsu Province 214122, P. R. China

[e] N. Van Steerteghem, Prof. K. Clays  
Laboratory of Chemical and Biological Dynamics,  
Centre for Research on Molecular Electronics and Photonics,  
Katholieke Universiteit Leuven, Celestijnenlaan 200D,  
B-3001 Leuven, Belgium

[†] Dedicated to the memory of Prof. Leone Spiccia.

[\*\*] Organometallic Complexes for Nonlinear Optics. Part 62. Part 61: J. Du, M. S. Kodikara, G. J. Moxey, M. Morshedi, A. Barlow, C. Quintana, G. Wang, R. Stranger, C. Zhang, M. P. Cifuentes, M. G. Humphrey, *Dalton Trans.*, accepted 15/2/18. Paper no DT-ART-01-2018-000155.

Supporting information and the ORCID identification numbers for the authors of this article can be found under  
<http://dx.doi.org/10.1002/xxx>.

## Introduction

Materials possessing nonlinear optical (NLO) properties that can modify the propagation characteristics of light (e.g. frequency, phase, path, etc) are urgently needed for applications in current and prospective photonics-based technologies. NLO-active organometallic complexes have consequently attracted significant interest.<sup>[1]</sup> In a similar fashion to organic molecules,<sup>[2]</sup> the NLO effects in organometallic complexes usually stem from polarization of the  $\pi$ -electron density. However, in comparison to organic molecules, organometallic complexes possess far greater flexibility in molecular design, and thereby the opportunity to tune and optimize NLO responses, while the reversible redox behavior exhibited by many metal complexes affords a facile means to potentially switch NLO output.<sup>[3]</sup>

The archetypical design for a quadratic NLO-active molecule, namely a donor- $\pi$ -bridge-acceptor (D-B-A) composition, has been the major focus of research into organometallic NLO materials. The most popular classes have been ferrocenyl complexes,<sup>[4]</sup> which exhibit enhanced stability compared to other organometallics, but for which the metal-to-cyclopentadienyl charge transfer is orthogonal to the charge transfer involving the chromophore appended to a cyclopentadienyl ring, and metal alkynyl complexes,<sup>[5]</sup> in which the metal-to-ligand charge transfer is in the plane of the chromophore, a potentially more-favourable arrangement.<sup>[6]</sup> Metal alkynyl complexes can exhibit large values of quadratic molecular optical nonlinearity, with resonant values

## FULL PAPER

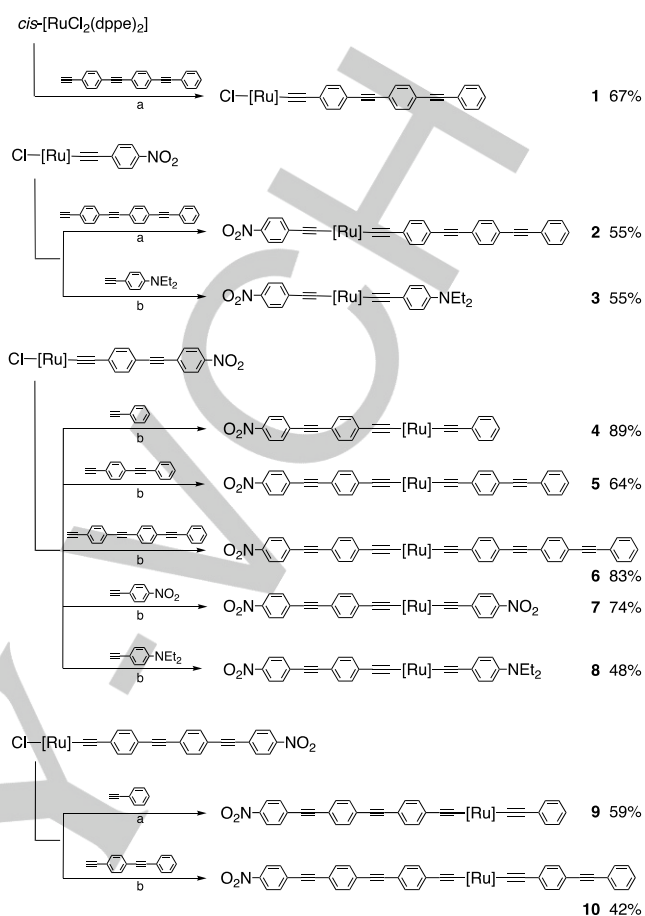
up to  $5000 \times 10^{-30}$  esu and frequency-independent values up to  $800 \times 10^{-30}$  esu being reported,<sup>[7]</sup> although the validity of the two-level model<sup>[8]</sup> being used to derive the frequency-independent data for these large molecules is highly questionable. Note that, in the more efficient examples, the ligated metal center has invariably functioned as the donor group in the classic D-B-A construction.

Metal alkynyl complexes have also attracted attention as potential cubic NLO-active materials, with the focus largely on complexes with extended  $\pi$ -systems such as cruciforms,<sup>[9]</sup> stars,<sup>[10]</sup> oligomers,<sup>[11]</sup> and dendrimers,<sup>[12]</sup> and with examples displaying record values of multi-photon absorption cross-sections.<sup>[13]</sup> The nonlinear refraction and nonlinear absorption coefficients are strongly wavelength-dependent. Many ligated metal centers quench fluorescence, rendering evaluation of multi-photon absorption (MPA) exploiting MPA-excited fluorescence impossible. The Z-scan technique has therefore been used, but the required spectral dependence studies are time-consuming, and metal alkynyl examples are limited (see, for example, references [9], 10, 11b, 11c, 12a, 13, 14).

The necessity of appending the ligated metal donor group to the terminus of a D-B-A construction has been assumed, but thus far, no systematic study exploring the outcome of locating the electron-rich bis(diphosphine)ruthenium center away from the OPE termini has appeared, which is a prerequisite to test this assumption. In addition, and as mentioned above, almost all studies exploring the wavelength dependence of cubic NLO properties in ruthenium alkynyl complexes have examined systems with multiple metal centers. To address these deficiencies, we report herein the syntheses of a range of complexes consisting of an oligo(*p*-phenyleneethynylene) (OPE) unit end-functionalized with an electron accepting nitro group and with a bis(diphosphine)ruthenium moiety at varying locations in the OPE structure, together with a comprehensive study of their linear optical, quadratic nonlinear optical, cubic nonlinear optical, electrochemical, and spectroelectrochemical behaviour, and theoretical studies aimed at rationalizing the experimental outcomes.

## Results and Discussion

**Synthesis.** The new mono(alkynyl)ruthenium complex *trans*-[Ru(C≡C-1,4-C<sub>6</sub>H<sub>4</sub>C≡C-1,4-C<sub>6</sub>H<sub>4</sub>C≡CPh)Cl(dppe)<sub>2</sub>] (**1**) (dppe = 1,2-bis(diphenylphosphino)ethane) and the new bis(alkynyl)ruthenium complexes *trans*-[Ru{(C≡C-1,4-C<sub>6</sub>H<sub>4</sub>)<sub>n</sub>NO<sub>2</sub>}(C≡CR)(dppe)<sub>2</sub>] (*n* = 1, R = 1,4-C<sub>6</sub>H<sub>4</sub>C≡C-1,4-C<sub>6</sub>H<sub>4</sub>C≡CPh (**2**), 1,4-C<sub>6</sub>H<sub>4</sub>NEt<sub>2</sub> (**3**); *n* = 2, R = Ph (**4**), 1,4-C<sub>6</sub>H<sub>4</sub>C≡CPh (**5**), 1,4-C<sub>6</sub>H<sub>4</sub>C≡C-1,4-C<sub>6</sub>H<sub>4</sub>C≡CPh (**6**), 1,4-C<sub>6</sub>H<sub>4</sub>NO<sub>2</sub> (**7**), 1,4-C<sub>6</sub>H<sub>4</sub>NEt<sub>2</sub> (**8**); *n* = 3, R = Ph (**9**), 1,4-C<sub>6</sub>H<sub>4</sub>C≡CPh (**10**)) were synthesized by exploiting established methodologies for the preparation of mono- and bis(alkynyl) complexes<sup>[15]</sup> (Scheme 1 and Supporting Information), and were characterized by a combination of IR, <sup>1</sup>H, <sup>13</sup>C, and <sup>31</sup>P NMR spectroscopies and mass spectrometry. The <sup>31</sup>P NMR spectrum of the mono(alkynyl)ruthenium complex **1** shows a singlet at 49.1 ppm, confirming the *trans*-stereochemistry of the complex. Similarly, the <sup>31</sup>P NMR spectra of the bis(alkynyl)ruthenium complexes **2-10**



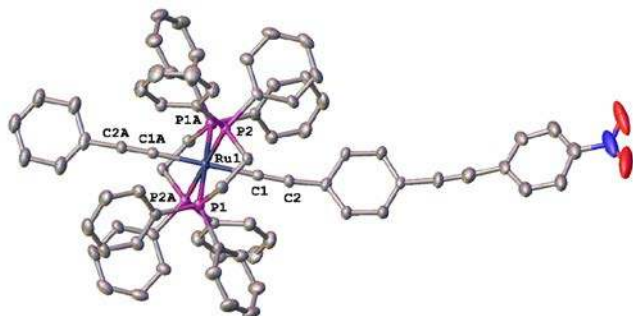
**Scheme 1.** Preparation of ruthenium alkynyl complexes **1-10**. [Ru] = *trans*-Ru(dppe)<sub>2</sub>; a) KPF<sub>6</sub>, CH<sub>2</sub>Cl<sub>2</sub>, NEt<sub>3</sub>; b) NaPF<sub>6</sub>, CH<sub>2</sub>Cl<sub>2</sub>, NEt<sub>3</sub>.

contain one singlet peak (53.1 – 54.5 ppm), as expected for *trans*-configuration. Mass spectra of the bis(alkynyl)ruthenium complexes **2-10** show molecular ions. While a molecular ion was not observed in the mass spectrum of **1**, a product ion corresponding to the replacement of the chloro ligand of the molecular ion by acetonitrile was seen. IR data show bands between 2039 and 2060 cm<sup>-1</sup> corresponding to the stretching frequencies of the ruthenium-bound C≡C unit. The identities of *trans*-[Ru(C≡C-1,4-C<sub>6</sub>H<sub>4</sub>C≡C-1,4-C<sub>6</sub>H<sub>4</sub>NO<sub>2</sub>)(C≡CPh)(dppe)<sub>2</sub>] (**4**) and *trans*-[Ru(C≡CPh)Cl(dppe)<sub>2</sub>] (**14**) were confirmed by single-crystal X-ray diffraction studies (Figure 1 and Figure S1, respectively), the latter a solvomorph of a previously reported crystal structure.<sup>[16]</sup>

**Electrochemical Studies.** The electrochemical properties of ruthenium alkynyl complexes have attracted considerable interest.<sup>[14c,14j,17]</sup> Table 1 summarizes results of cyclic voltammetric studies for ruthenium alkynyl complexes **1-10**, together with data acquired simultaneously from the related complexes **14-18**; data for **11-14** have been reported previously and those for **14** are in agreement with the present data.<sup>[18,19]</sup> It is widely accepted that the HOMO in such ruthenium alkynyl

## FULL PAPER

complexes has considerable contribution from the metal-adjacent phenylalkynyl group, in addition to the expected metal



**Figure 1.** Molecular structure of **4**, with thermal ellipsoids set at the 40% probability level. Hydrogen atoms and the disordered components of the alkyne ligands have been omitted for clarity. Selected bond lengths (Å) and angles (°): Ru1-C1 2.066(3), Ru1-C1A 2.066(3), Ru1-P1 2.3581(9), Ru1-P1A 2.3582(9), Ru1-P2 2.3657(12), Ru1-P2A 2.3657(12), C1-C2 1.213(4), C1-Ru-C1A 180.0, C1-Ru1-P1 89.45(8), C1-Ru1-P1A 90.55(8), C1-Ru1-P2 98.41(8), C1-Ru1-P2A 81.59(8), C1A-Ru1-P1 90.55(8), C1A-Ru1-P1A 89.45(8), C1A-Ru1-P2 81.59(8), C1A-Ru1-P2A 98.41(8), P1-Ru1-P1A 180.0, P1-Ru1-P2 81.89(3), P1-Ru1-P2A 98.11(3), P1A-Ru1-P2 98.11(3), P1A-Ru1-P2A 81.89(3), P2-Ru1-P2A 180.0. Symmetry operation used to generate equivalent atoms, A: 1-x, 1-y, -z.

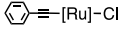
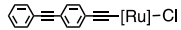
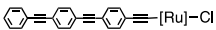
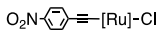
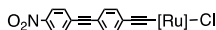
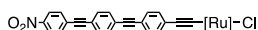
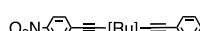



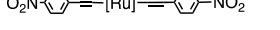
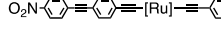
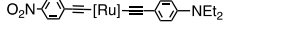
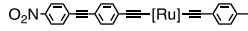
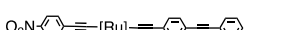



character,<sup>[14j,19]</sup> but for conciseness we have labeled the first oxidation processes as Ru<sup>II/III</sup>; we emphasize that this simplification should be borne in mind. The Ru<sup>II/III</sup> oxidation processes for the non-functionalized (chloro)alkynyl complexes are typically reversible, occurring at potentials of ca. 0.55 V and invariant on  $\pi$ -system lengthening by addition of further phenyleneethynylene units (proceeding from **14** to **15** and then to **1**). In the complexes containing functionalized phenyl groups, oxidation of the NEt<sub>2</sub> group occurs at ca. 0.75 V (**3** and **8**), and cathodic waves are found for the NO<sub>2</sub> reduction process (-0.84 – -1.16 V) with the exception of the di-nitro complex **18**, which displays a single irreversible nitro-centered reduction process (-1.17 V). Analysis of trends in the data affords information on modulation of the electron density resultant from (i) introduction and structural modification of the second alkyne ligand, and (ii)  $\pi$ -bridge lengthening. Specifically, replacing a chloro ligand with a phenylethynyl ligand leads to a decrease in the Ru<sup>II/III</sup> oxidation potential, consistent with increased electron density around the metal from the strong  $\sigma$ -bonding alkyne ligand; this effect diminishes as the length of the nitro-functionalized alkyne ligand increases, and thereby its electron-depleting effect decreases (proceeding from **11** to **16**, **12** to **4**, or **13** to **9**). Replacing a chloro ligand with an amino-functionalized alkyne ligand results in a significant decrease in Ru<sup>II/III</sup> oxidation potential to ca. 0.27 V (**11** to **3**, **12** to **8**). Extending the non-nitro-functionalized alkyne ligand while keeping the nitro-functionalized alkyne ligand invariant leads to negligible change in the oxidation potential (**16** to **17** to **2**, **4** to **5** to **6**, or **9** to **10**). In contrast, extending the nitro-functionalized alkyne ligand while keeping the non-functionalized alkyne ligand invariant generally affords a decrease in metal-centered oxidation potential on proceeding from mono- to bis-phenyleneethynylene-containing bridge, but lengthening to a tri(phenyleneethynylene) bridge results in negligible further change (**16** to **4** to **9**, **17** to **5** to **10**, **2** to **6**). In general, the impact on the metal-centered oxidation potential of the functional groups diminishes as their location moves from the phenyl ring adjacent

to the metal to the second phenyl ring (counting from the metal center), while at the third ring, the functional groups no longer exert a significant influence on the metal-centered oxidation potential.

**Optical Properties.** The intense low-energy bands in the linear optical spectra of ruthenium mono(alkynyl) complexes of this type have been assigned previously as metal-to-ligand charge transfer (MLCT) in character.<sup>[14d,14j,17c,17f]</sup> In the present study, we have explored the dependence of the wavelength of the optical absorption maxima on the nature of the alkyne ligands, the data for **1-18** being collected in Table 1, and the trends upon certain structural modifications being illustrated in Figures 2-5. We and others have previously noted that  $\pi$ -bridge lengthening of a nitro-functionalized alkyne ligand by adding phenyleneethynylene units (e.g. in proceeding from **11** to **12** and then to **13**) results in a blue shift in absorption maximum,<sup>[14d,17f,20]</sup> mimicking the trend seen with purely organic dipolar molecules.<sup>[21]</sup> A similar trend is seen in the present work, in proceeding from **16** to **4** and then **9**, and also in proceeding from **17** to **5** and then **10** (Figure 3). The systematically-varied series of complexes listed in Table 1 enable additional structure-property observations to be made. Replacing a chloro ligand with a phenylethynyl ligand leads to a red shift in  $\lambda_{\text{max}}$  and gives rise to a new band at higher energy, or causes a red shift in the second lowest energy band, as in proceeding from **11** to **16** (Figure 2), **12** to **4** or **13** to **9**.  $\pi$ -Bridge lengthening by inserting phenyleneethynylene units into the non-functionalized ligand while keeping the nitro-functionalized ligand invariant (proceeding from **16** to **17** (Figure 2), **17** to **2** (Figure 2), **4** to **5**, or **9** to **10**) leads to a weak blue shift in  $\lambda_{\text{max}}$  and a strong red shift in the second-lowest-energy band.  $\pi$ -Bridge lengthening by inserting phenyleneethynylene units into the nitro-functionalized alkyne ligand while keeping the non-functionalized alkyne ligand invariant (proceeding from **16** to **4**, **4** to **9**, **17** to **5** (Figure 3), or **5** to **10** (Figure 3)) leads to a blue shift in  $\lambda_{\text{max}}$  and a red shift in the second lowest energy band.  $\pi$ -Bridge lengthening by inserting phenyleneethynylene units into the nitro-functionalized alkyne ligand, while concomitantly decreasing the length of the non-functionalized alkyne ligand by the same number of phenyleneethynylene units (and thereby keeping the total length invariant or, alternatively, examining positional isomers) (proceeding from **17** to **4**, **2** to **5** (Figure 4), or **5** to **9** (Figure 4)) leads to a decrease in intensity in  $\lambda_{\text{max}}$  and a blue shift in the second lowest energy band. Replacing the chloro ligand with a 4-(diethylamino)phenylethynyl ligand (proceeding from **11** to **3** (Figure 5), or **12** to **8**) leads to a red shift in  $\lambda_{\text{max}}$  and gives rise to a new band at higher energy, while replacing the chloro ligand with a 4-nitrophenylethynyl ligand (proceeding from **11** to **18** or **12** to **7**) leads to a red shift in  $\lambda_{\text{max}}$ .

**Theoretical studies.** Time-dependent density functional theory (TD-DFT) calculations were used to rationalize the experimental linear optical data of **2-4**, **9**, **11**, **16-18**, and thereby to shed light on the spectra of all complexes in the present study and the trends delineated in the previous section. Studies were undertaken on the model complexes **2M-4M**, **9M**, **11M**, **16M-18M** (see Figure 6). A number of observations can be made by examining this systematically-varied suite of complexes. Firstly, the series **11M**, **16M**, **17M**, and **2M** afford the possibility of probing the effect of introducing and then extending the length of a non-functionalized

**Table 1.** Electrochemical and linear optical data and hyper-Rayleigh scattering-derived nonlinear optical response parameters.

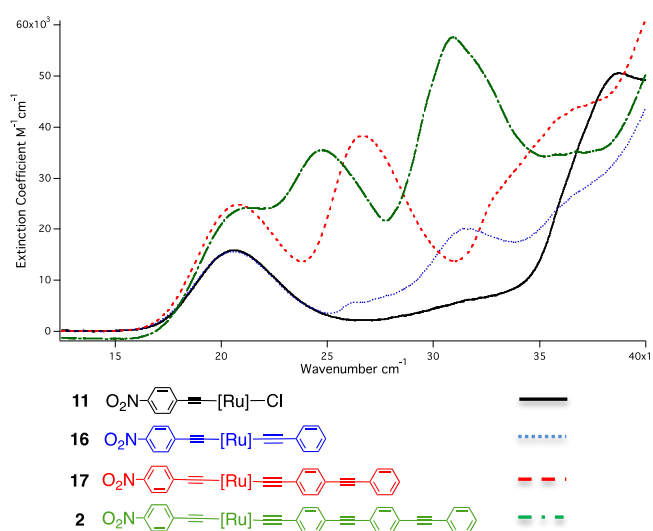
Complex <sup>[a]</sup>		$E_{\text{ox}}^0$ [b] [i <sub>pa</sub> /i <sub>pc</sub> ] Ru <sup>II/III</sup>	$E_{\text{red}}^0$ [b] [i <sub>pa</sub> /i <sub>pc</sub> ] NO <sub>2</sub> <sup>III/II</sup>	$\lambda_{\text{max}}$ [ε] [c]	$\beta_{1064}$ [d]	$\beta_0$ [e]	Reference
	<b>14</b>	0.55 [1]	-	320 [1.9]	39	23	This work
	<b>15</b>	0.55 [1]	-	387 [3.1]	99	40	This work
	<b>1</b>	0.55 [1]	-	415 [3.5]	227	75	This work
	<b>11</b>	0.74 [0.9]	-0.84 [0.8]	477 [2.0]	562 ± 9	88 ± 1	[19]
	<b>12</b>	0.60 [1]	-0.94 [0.9]	468 [1.8]	1240 ± 110	225 ± 20	[19]
	<b>13</b>	0.58 [1]	-0.91 [0.9]	435 [1.2]	1327 ± 110	388 ± 32	[19]
	<b>16</b>	0.64 [1]	-1.00 [1]	486 [1.3]	517	68	This work
	<b>4</b>	0.56 [1]	-0.94 [1]	472 [2.7]	802	137	This work
	<b>9</b>	0.56 [1]	-0.89 [0.9]	435 [1.9]	473	131	This work
	<b>18</b>	0.74 [1]	-1.17 [irr]	489 [2.0]	476	58	This work
	<b>7</b>	0.70 [1]	-0.93 [1]	483 [3.4]	507	71	This work
	<b>3</b> [f]	0.27 [1]	-1.16 [1]	500 [1.3]	577	52	This work
	<b>8</b> [g]	0.27 [1]	-0.93 [1]	477 [1.6]	809	127	This work
	<b>17</b>	0.67 [1]	-1.13 [1]	482 [2.2]	555	79	This work
	<b>5</b>	0.57 [1]	-0.94 [1]	470 [2.8]	732	129	This work
	<b>10</b>	0.56 [1]	-0.91 [0.8]	433 [3.5]	526	148	This work
	<b>2</b>	0.68 [1]	-1.08 [1]	474 [2.4]	526	87	This work
	<b>6</b>	0.56 [1]	-0.94 [1]	466 [2.0]	[h]	[h]	This work

[a] [Ru] = *trans*-Ru(dppe)<sub>2</sub>. [b] V, measured in CH<sub>2</sub>Cl<sub>2</sub>, FcH/FcH<sup>+</sup> E<sup>0</sup> = 0.56 V [22]. [c] nm [ε, 10<sup>4</sup> M<sup>-1</sup> cm<sup>-1</sup>]. [d] 10<sup>-30</sup> esu, values are ± 10% unless stated otherwise, measured in THF. [e] 10<sup>-30</sup> esu, measured in THF, corrected for resonance enhancement at 532 nm using the two-level model with  $\beta_0 = \beta[1 - (2\lambda_{\text{max}}/1064)^2][1 - (\lambda_{\text{max}}/1064)^2]$ . [f] E<sup>0</sup><sub>ox</sub> [i<sub>pa</sub>/i<sub>pc</sub>] NEt<sub>2</sub> = 0.76 [22]; [g] E<sup>0</sup><sub>ox</sub> [i<sub>pa</sub>/i<sub>pc</sub>] NEt<sub>2</sub> = 0.75 [22]. [h] not measured.

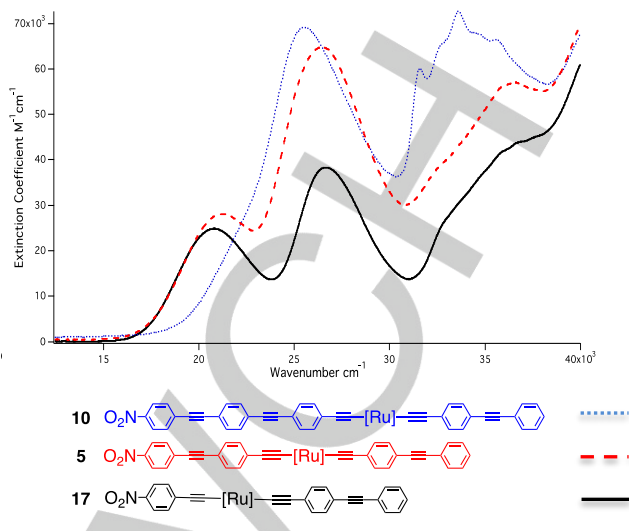
alkynyl ligand. Replacing the chloro ligand with a phenylethynyl ligand, on proceeding from **11M** to **16M**, results in a considerable red-shift in the lowest-energy transition arising from the HOMO to LUMO excitation, the HOMO being destabilized compared to the LUMO (Table 3). The HOMO → LUMO excitations in both **11M** and **16M** are admixtures of MLCT and ligand-to-ligand CT (LLCT) transitions (Figure 7). The experimental UV/Vis spectrum of **16** contains an intense transition at ca. 32,000 cm<sup>-1</sup>. Similarly, the TD-DFT data of **16M** also show an intense band at 33,700 cm<sup>-1</sup> resulting from the HOMO to LUMO+1 transition. Upon further extending the conjugation of the non-nitro functionalized alkynyl ligand, on proceeding from **16M** to **17M**, and then to **2M**, the HOMO → LUMO transition is essentially invariant (Table 2), but its intensity increases. The composition of the LUMO orbitals of **16M**, **17M**, and **2M** are approximately the same, being largely localized on the [C≡C-1,4-C<sub>6</sub>H<sub>4</sub>NO<sub>2</sub>] group (Figure 7). In contrast, the electron density of the HOMO leaks to the oligo(phenyleneethyne) bridge as the conjugation increases, so the calculated lowest-energy bands can be assigned as MLCT with considerable LLCT contribution. The HOMO → LUMO+1

transition red-shifts significantly with increasing conjugation because the LUMO+1 is increasingly stabilized (Table 3), consistent with the experimental observation of a red-shift in the second lowest-energy absorption band on proceeding from **16** to **17**, and then **2**. The LUMO+1 of **16M**, **17M**, and **2M** are localized on the non-nitro-containing alkynyl ligand (Figures S9, S10, and S4, respectively), so the HOMO → LUMO+1 excitation shows significant MLCT character. We note that the low-energy band computed at ca. 26,000 cm<sup>-1</sup> for **17M** has a contribution from the HOMO-2 → LUMO transition; the HOMO - LUMO+1 and HOMO-2 - LUMO energy gaps are approximately the same for **17M**, according to Table 3.

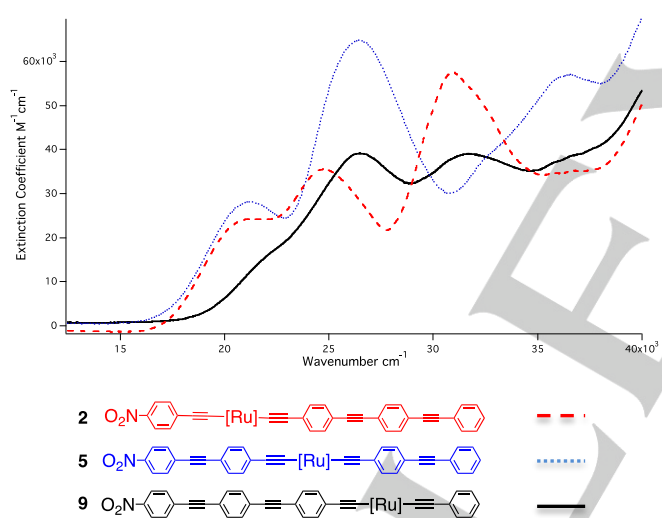
The effect of extending the length of the nitro-functionalized ligand was also explored, from considering the series **16M**, **4M**, and **9M**. Extending the length of the nitro-functionalized ligand, on proceeding from **16M** to **4M**, leads to a considerable red-shift in the HOMO → LUMO transition, but further increase in the conjugation (proceeding from **4M** to **9M**) has little effect on the excitation energy (Table 2), consistent with the relative  $\Delta_{\text{H-L}}$  values in Table 3 (i.e. **16M** >> **4M** > **9M**). The HOMO → LUMO



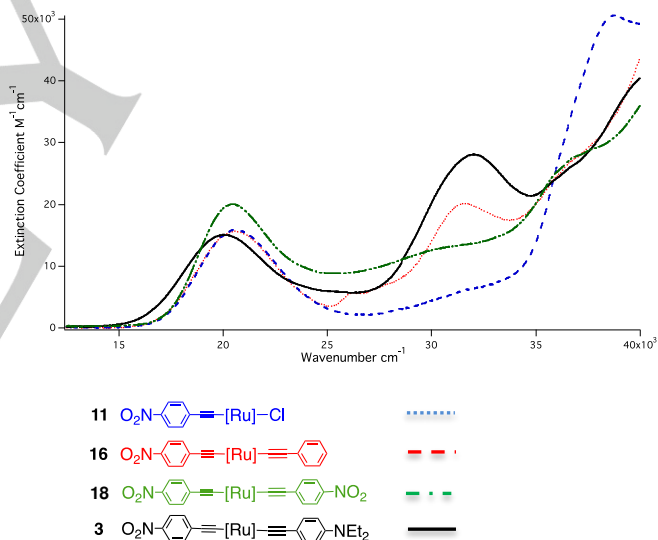
**Figure 2.** Optical spectra of *trans*-[Ru(C≡C-1,4-C<sub>6</sub>H<sub>4</sub>NO<sub>2</sub>)Cl(dppe)<sub>2</sub>] (**11**), *trans*-[Ru(C≡C-1,4-C<sub>6</sub>H<sub>4</sub>NO<sub>2</sub>)(C≡CPh)(dppe)<sub>2</sub>] (**16**), *trans*-[Ru(C≡C-1,4-C<sub>6</sub>H<sub>4</sub>NO<sub>2</sub>)(C≡C-1,4-C<sub>6</sub>H<sub>4</sub>C≡CPh)(dppe)<sub>2</sub>] (**17**), and *trans*-[Ru(C≡C-1,4-C<sub>6</sub>H<sub>4</sub>NO<sub>2</sub>)(C≡C-1,4-C<sub>6</sub>H<sub>4</sub>C≡C-1,4-C<sub>6</sub>H<sub>4</sub>C≡CPh)(dppe)<sub>2</sub>] (**2**).



**Figure 3.** Optical spectra of *trans*-[Ru(C≡C-1,4-C<sub>6</sub>H<sub>4</sub>C≡C-1,4-C<sub>6</sub>H<sub>4</sub>C≡C-1,4-C<sub>6</sub>H<sub>4</sub>NO<sub>2</sub>)(C≡C-1,4-C<sub>6</sub>H<sub>4</sub>C≡CPh)(dppe)<sub>2</sub>] (**10**), *trans*-[Ru(C≡C-1,4-C<sub>6</sub>H<sub>4</sub>C≡C-1,4-C<sub>6</sub>H<sub>4</sub>NO<sub>2</sub>)(C≡C-1,4-C<sub>6</sub>H<sub>4</sub>C≡CPh)(dppe)<sub>2</sub>] (**5**), and *trans*-[Ru(C≡C-1,4-C<sub>6</sub>H<sub>4</sub>NO<sub>2</sub>)(C≡C-1,4-C<sub>6</sub>H<sub>4</sub>C≡CPh)(dppe)<sub>2</sub>] (**17**).



**Figure 4.** Optical spectra of *trans*-[Ru(C≡C-1,4-C<sub>6</sub>H<sub>4</sub>NO<sub>2</sub>)(C≡C-1,4-C<sub>6</sub>H<sub>4</sub>C≡C-1,4-C<sub>6</sub>H<sub>4</sub>C≡CPh)(dppe)<sub>2</sub>] (**2**), *trans*-[Ru(C≡C-1,4-C<sub>6</sub>H<sub>4</sub>C≡C-1,4-C<sub>6</sub>H<sub>4</sub>NO<sub>2</sub>)(C≡C-1,4-C<sub>6</sub>H<sub>4</sub>C≡CPh)(dppe)<sub>2</sub>] (**5**), and *trans*-[Ru(C≡C-1,4-C<sub>6</sub>H<sub>4</sub>C≡C-1,4-C<sub>6</sub>H<sub>4</sub>C≡C-1,4-C<sub>6</sub>H<sub>4</sub>NO<sub>2</sub>)(C≡CPh)(dppe)<sub>2</sub>] (**9**).



**Figure 5.** Optical spectra of *trans*-[Ru(C≡C-1,4-C<sub>6</sub>H<sub>4</sub>NO<sub>2</sub>)Cl(dppe)<sub>2</sub>] (**11**), *trans*-[Ru(C≡C-1,4-C<sub>6</sub>H<sub>4</sub>NO<sub>2</sub>)(C≡CPh)(dppe)<sub>2</sub>] (**16**), *trans*-[Ru(C≡C-1,4-C<sub>6</sub>H<sub>4</sub>NO<sub>2</sub>)(C≡C-1,4-C<sub>6</sub>H<sub>4</sub>NO<sub>2</sub>)(dppe)<sub>2</sub>] (**18**), and *trans*-[Ru(C≡C-1,4-C<sub>6</sub>H<sub>4</sub>NO<sub>2</sub>)(C≡C-1,4-C<sub>6</sub>H<sub>4</sub>NEt<sub>2</sub>)(dppe)<sub>2</sub>] (**3**).

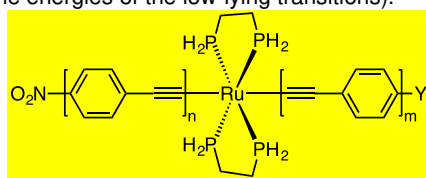
transition in **4M** and **9M** results from an admixture of MLCT [ $d(\text{Ru}) \rightarrow \pi^*(1,4\text{-C}_6\text{H}_4\text{NO}_2)$ ], LLCT [ $\pi(\text{C}\equiv\text{CPh}) \rightarrow \pi^*(1,4\text{-C}_6\text{H}_4\text{NO}_2)$ ], and intraligand CT (ILCT, within the nitro-functionalized ligand) transitions, according to Figure 7. Two higher-energy transitions (HOMO-2  $\rightarrow$  LUMO and HOMO  $\rightarrow$  LUMO+1) are also red-shifted; the shifts become more pronounced with increasing conjugation length compared to that of the HOMO  $\rightarrow$  LUMO excitation. Several transitions close in energy were found for **9M** below  $30,000 \text{ cm}^{-1}$ , perhaps explaining the relatively broad absorption profile in the experimental UV/Vis spectrum of **9**.

However, the calculations do not explain the experimental blue-shift in the lowest-energy absorption band on proceeding from **16** to **4** to **9**, which is clearly more pronounced than the blue-shift found on proceeding from **16** to **17** to **2**. Long-range corrections were needed to successfully reproduce the blue-shift in the low-lying UV/Vis bands observed experimentally upon elongation of the  $\pi$ -bridge in related Fe complexes.<sup>[20b]</sup> The lowest-energy  $S_0 \rightarrow S_1$  transitions for **2M**, **4M**, **9M**, **16M**, and **17M** were consequently recalculated with the B3LYP and CAM-B3LYP<sup>[23]</sup> functionals (Table S1: CAM-B3LYP is the long-range corrected version of

**Table 2.** TD-DFT studies of the model complexes. First 30 singlet states were calculated. Only transitions with oscillator strengths ( $f$ ) greater than 0.3 are reported. Wavenumbers ( $\nu$ ) are in  $\text{cm}^{-1}$ .

Complex	State	$\nu$	$f$	Major contribution (%)
<b>2M</b>	S <sub>1</sub>	20500	1.113	HOMO → LUMO (94)
	S <sub>3</sub>	23200	1.547	HOMO → LUMO+1 (91)
	S <sub>6</sub>	28200	0.931	HOMO-2 → LUMO+1 (89)
<b>3M</b>	S <sub>1</sub>	18700	0.357	HOMO → LUMO (99)
	S <sub>3</sub>	24800	0.507	HOMO-2 → LUMO (98)
	S <sub>13</sub>	34000	0.770	HOMO → LUMO+3 (84)
<b>4M</b>	S <sub>1</sub>	17800	0.724	HOMO → LUMO (98)
	S <sub>3</sub>	23200	0.505	HOMO-2 → LUMO (97)
	S <sub>4</sub>	27800	0.838	HOMO → LUMO+1 (91)
	S <sub>15</sub>	33700	0.467	HOMO → LUMO+3 (78)
<b>9M</b>	S <sub>1</sub>	17200	0.646	HOMO → LUMO (97)
	S <sub>3</sub>	21900	1.009	HOMO-2 → LUMO (88)
	S <sub>4</sub>	24000	0.841	HOMO → LUMO+1 (88)
	S <sub>5</sub>	26500	0.388	HOMO-3 → LUMO (89)
	S <sub>7</sub>	29200	0.367	HOMO-2 → LUMO+1 (92)
<b>11M</b>	S <sub>12</sub>	31600	0.354	HOMO → LUMO+2 (85)
	S <sub>2</sub>	22500	0.694	HOMO → LUMO (99)
<b>16M</b>	S <sub>1</sub>	20800	0.568	HOMO → LUMO (99)
	S <sub>3</sub>	27000	0.334	HOMO-2 → LUMO (98)
	S <sub>10</sub>	33700	0.601	HOMO → LUMO+1 (92)
<b>17M</b>	S <sub>1</sub>	20600	0.734	HOMO → LUMO (97)
	S <sub>3</sub>	26000	1.271	HOMO-2 → LUMO (55); HOMO → LUMO+1 (40)
	S <sub>10</sub>	32400	0.509	HOMO-2 → LUMO+1 (89)
<b>18M</b>	S <sub>1</sub>	21200	1.201	HOMO → LUMO (98)
	S <sub>6</sub>	28900	0.438	HOMO-2 → LUMO+1 (98)

B3LYP). However, in contrast to the aforementioned study with iron complexes, all three methods yielded a red-shift in the S<sub>0</sub> → S<sub>1</sub> transition upon extension of either of the axial ligands in **16M** (indeed, excitation energies are method-dependent, and the CAM-B3LYP functional was found to significantly overestimate the energies of the low-lying transitions).



**Figure 6.** Model complexes used in the computational studies.

<b>2M</b>	$n = 1, Y = H, m = 3$	<b>11M</b>	$n = 1, Y = Cl, m = 0$
<b>3M</b>	$n = 1, Y = NH_2, m = 1$	<b>16M</b>	$n = 1, Y = H, m = 1$
<b>4M</b>	$n = 2, Y = H, m = 1$	<b>17M</b>	$n = 1, Y = H, m = 2$
<b>9M</b>	$n = 3, Y = H, m = 1$	<b>18M</b>	$n = 1, Y = NO_2, m = 1$

Low-energy linear optical behaviour is expected to be significantly affected by planarity of the  $\pi$ -bridge, as shown by previous related studies.<sup>[11b,14d,19,24]</sup> We assessed the influence of the orientation of the alkyne ligands with respect to the metal center, as well as the relative orientation of the planes of the two alkyne ligands, on the low-lying linear optical data in **16M**, the smallest bis(alkynyl) complex in the set. A two-dimensional potential energy scan was performed on **16M**, details of which are provided in the Supporting Information (Figures S2 and S3). TD-DFT studies were undertaken on a few selected points on the surface; convoluted UV/Vis spectra are shown in Figure 8 for selected rotamers.

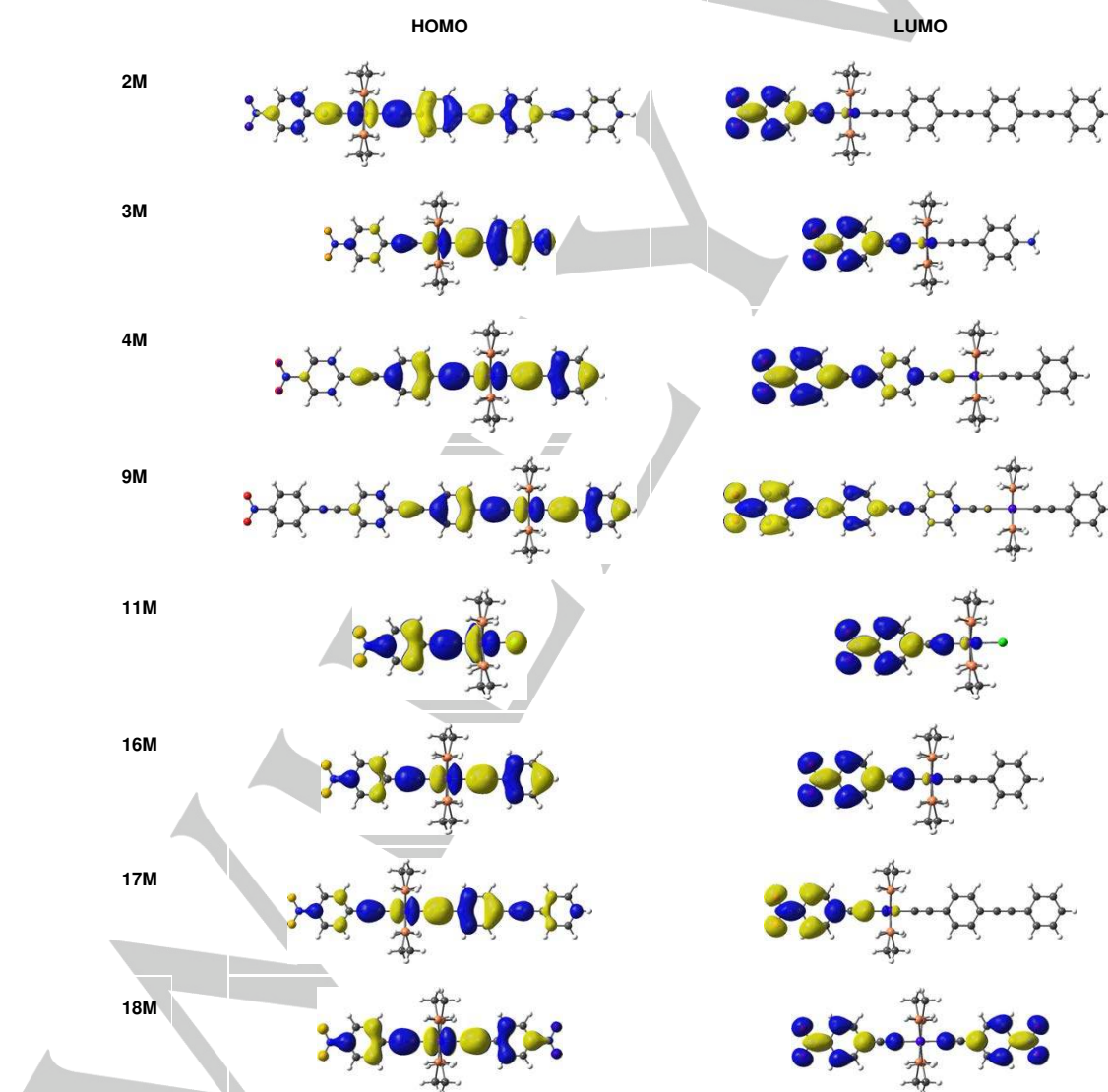
The barriers to rotation in **16M** of the nitro-functionalized phenylene group (with respect to the metal center) as well as that of the non-functionalized phenyl (with respect to the nitro-functionalized phenylene) were found to be very small (see Figure S3), suggesting that a wide range of conformations are in equilibrium with the coplanar structures under the experimental condition. Figure 8 shows how the low-lying linear optical data is affected by the orientation of the aryl groups in **16M**. It is clear that the oscillator strength of the high-energy transition increases dramatically with respect to that of its low-energy neighbour, the HOMO → LUMO transition, upon twisting the arylalkynyl ligands out of coplanarity. This, in turn, leads to a blue-shift in the convoluted lowest-energy bands of the twisted forms. It is anticipated that this should also hold for other bis(alkynyl) complexes, e.g. **17M** and **4M**. Note that **17M** and **4M** have two or more aryl groups in one of their alkyne ligands, and the addition of the extra aryl groups will increase the number of probable (twisted) conformations at ambient temperature. Each extra ring, distal to Ru, can rotate around the C<sub>sp</sub>-C<sub>sp</sub><sup>2</sup> bond and the barrier to such rotation is generally small.<sup>[24]</sup> As previously shown,<sup>[14d]</sup> the internal rotation of the phenylene groups along the axis of the triple bonds in an alkyne ligand can also contribute to the experimental observation of a blue-shift in the low-energy absorption band upon  $\pi$ -system lengthening. The experimental blue-shift in the lowest-energy absorption band in chromophores with long axial ligands probably results from internal rotations of the aryl groups in both alkyne ligands.

The influence of the electron-donating or -withdrawing characteristics of the alkyne ligand *trans* to the 1-nitrophenyl-4-ethynyl ligand was also probed. Replacing the chloro ligand with an amino-functionalized phenylethynyl ligand, on proceeding from **11M** to **3M**, results in an increase in the HOMO energy (Table 3). This leads to a substantially red-shifted HOMO → LUMO transition in **3M** (Table 2). This trend is consistent with the experimental data (Figure 5), although the red-shift is more profound in the calculations. The HOMO → LUMO and HOMO-2 → LUMO transitions in **3M** show an admixture of MLCT and LLCT character (Figure 7 and S5). A red-shift in the HOMO → LUMO transition is predicted when the chloro ligand in **11M** is replaced by the 1-nitrophenyl-4-ethynyl ligand in **18M**, in very good agreement with the experimental observation; the red-shift results from a smaller HOMO-LUMO energy gap for **18M** compared to that of **11M**. In **18M**, the axial ligands are identical, and so the electron density of the HOMO and LUMO are equally distributed on the nitro-functionalized ligands, with ruthenium making a significant contribution to the HOMO (Figure 7); the HOMO → LUMO transition in **18M** therefore has substantial MLCT character.

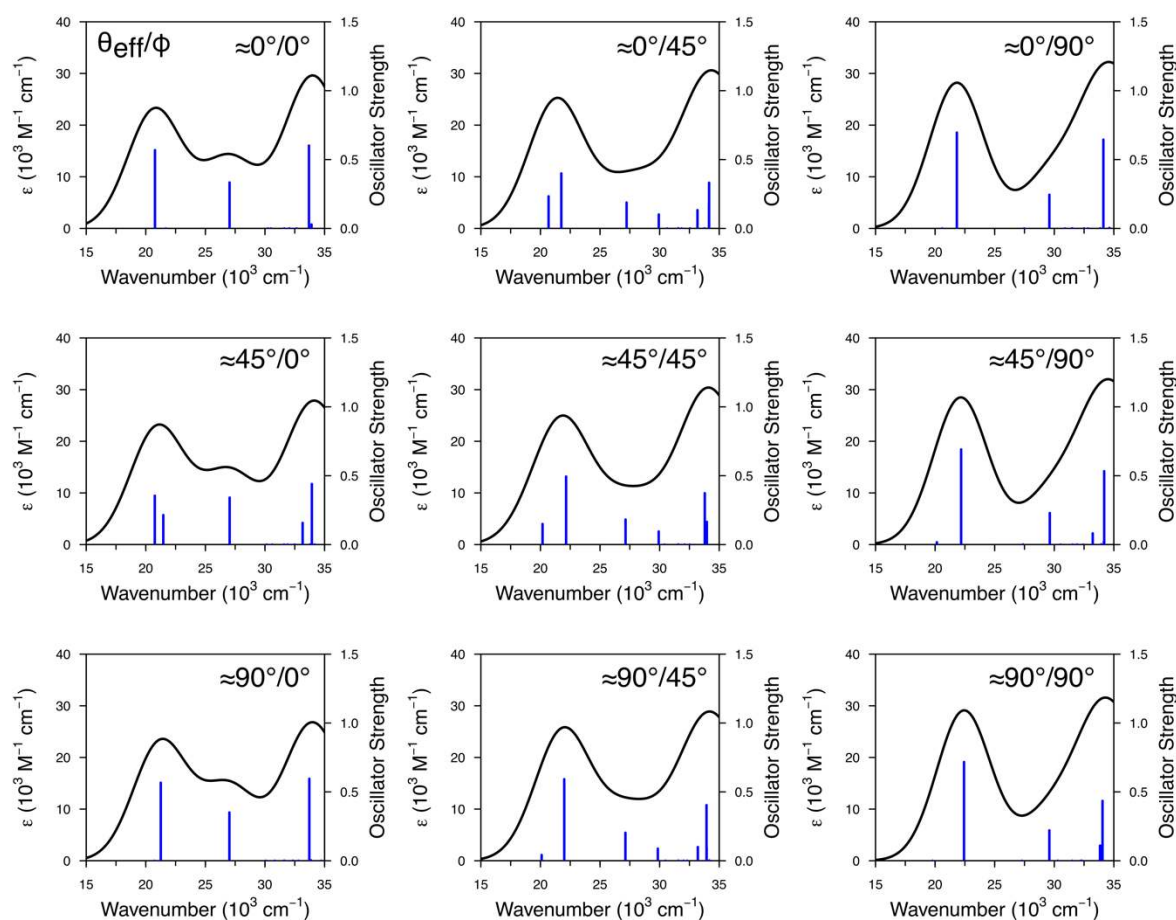
**Spectroelectrochemical studies.** In situ UV/Vis/NIR spectroelectrochemical studies using an optically transparent thin-layer electrochemical (OTTLE) cell allow simultaneous collection of spectra while the complex is undergoing a redox process. Application of suitable potentials to dichloromethane solutions of selected complexes afforded clean isosbestic points during the formally Ru<sup>II</sup> to Ru<sup>III</sup> oxidation process; a representative example is given in Figure 9, and pertinent results are collected in Table 4. Previous theoretical studies have assigned the lowest energy band (7,000-15,000 cm<sup>-1</sup>) in the spectra of related oxidized complexes as ligand-to-metal charge transfer (LMCT) in character.<sup>[19,25]</sup> Examination of the spectral data of the oxidized complexes in this study affords several conclusions.  $\pi$ -System lengthening leads to a red shift in the key lowest energy band (proceeding from 11<sup>+</sup> to 12<sup>+</sup> and on to 13<sup>+</sup>, and from 14<sup>+</sup> to 15<sup>+</sup>),

**Table 3.** Molecular orbital energies and HOMO–LUMO gaps ( $\Delta_{H-L}$ ). All values in eV.

Orbital	2M	3M	4M	9M	11M	16M	17M	18M
LUMO+3	-0.553	-0.308	-0.543	-0.858	-0.412	-0.342	-0.369	-0.576
LUMO+2	-1.067	-0.312	-0.796	-0.922	-0.418	-0.538	-0.550	-0.586
LUMO+1	-2.117	-0.522	-1.416	-1.945	-0.540	-0.590	-1.653	-2.467
<b>LUMO</b>	<b>-2.502</b>	<b>-2.472</b>	<b>-2.834</b>	<b>-2.937</b>	<b>-2.483</b>	<b>-2.487</b>	<b>-2.498</b>	<b>-2.572</b>
<b>HOMO</b>	<b>-5.443</b>	<b>-5.142</b>	<b>-5.350</b>	<b>-5.310</b>	<b>-5.726</b>	<b>-5.466</b>	<b>-5.445</b>	<b>-5.678</b>
HOMO–1	-5.895	-5.785	-5.783	-5.765	-6.007	-5.839	-5.887	-5.979
HOMO–2	-6.061	-5.979	-6.039	-5.947	-7.003	-6.273	-6.141	-6.501
HOMO–3	-6.528	-6.816	-6.818	-6.593	-7.136	-6.878	-6.878	-7.032
$\Delta_{H-L}$	<b>2.941</b>	<b>2.670</b>	<b>2.516</b>	<b>2.373</b>	<b>3.243</b>	<b>2.980</b>	<b>2.947</b>	<b>3.107</b>

**Figure 7.** Isosurface plots of HOMO and LUMO orbitals of model complexes investigated in this work. A complete set of molecular orbitals involved in the main transitions listed in Table 2 is provided in the Supporting Information (Figures S5–S12).





**Figure 8.** Effect of coplanarity of the axial ligands on the low-energy linear optical spectral region of **16M**.  $\theta_{\text{eff}}$  is the dihedral angle between the plane bisecting the  $\text{H}_2\text{PCH}_2\text{CH}_2\text{PH}_2$  bite angle and the plane of the nitro-functionalized alkynyl ligand.

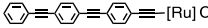
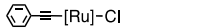
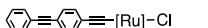
and a red shift is also observed upon replacing the chloro ligand with an alkynyl ligand (proceeding from **11**<sup>+</sup> to **17**<sup>+</sup> or **3**<sup>+</sup>, and proceeding from **12**<sup>+</sup> to **7**<sup>+</sup> or **8**<sup>+</sup>). Introducing a nitro group at the *para* position of the phenylethynyl ligand leads to a red shift in the absorption maximum (proceeding from **14**<sup>+</sup> to **11**<sup>+</sup>), but results in a blue shift if introduced at the most remote site (with respect to the location of the metal) of more extended arylalkynyl ligands (proceeding from **15**<sup>+</sup> to **12**<sup>+</sup>).

In the case of the diethylamino-containing complexes **3** and **8**, the fully reversible  $\text{Ru}^{\text{IV/III}}$  oxidation processes are accompanied by reversible oxidation processes at higher potentials that were assigned to the  $\text{NEt}_2^{0/1}$  process, with the distinct optical changes rendering these complexes possible candidates for multi-state switching applications.<sup>[9,17]</sup>

IR spectral data for complexes **1**, **14**, **15**, and their oxidation products are listed in Table 5. Oxidation of dichloromethane solutions of each complex at a ca. 0.2 V more positive potential than that of the  $\text{Ru}^{\text{IV/III}}$  process resulted in the disappearance of the band located at ca. 2060  $\text{cm}^{-1}$  associated with the symmetric

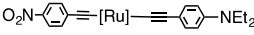
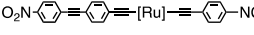
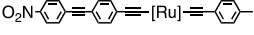
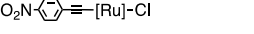
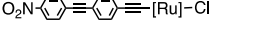
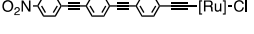
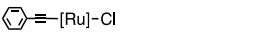
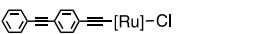
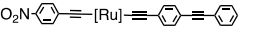
$\nu(\text{C}\equiv\text{C})$  stretching mode, and the concomitant appearance of a band at ca. 1905  $\text{cm}^{-1}$ . The redox process is reversible, with the band at ca. 2060  $\text{cm}^{-1}$  reappearing on application of a sufficiently negative potential.

**Table 5.** IR spectroelectrochemical data for **1**, **14** and **15**.<sup>a</sup>

Complex	$\nu(\text{MC}\equiv\text{C})$ $\text{cm}^{-1}$	
	[M]	[M] <sup>+</sup>
 <b>1</b>	2065	1901
 <b>14</b>	2070	1909
 <b>15</b>	2059	1904

<sup>a</sup> Data were collected at room temperature in  $\text{CH}_2\text{Cl}_2$  using a cell containing Pt grid working, Pt auxiliary and Ag/AgCl reference electrodes.

**Table 4.** UV/Vis/NIR spectroelectrochemical data for selected complexes.<sup>[a]</sup>

Complex ([M])	[M]		[M] <sup>+</sup>		[M] <sup>2+</sup>	
	V <sub>max</sub> , cm <sup>-1</sup> [ε, 10 <sup>4</sup> M <sup>-1</sup> cm <sup>-1</sup> ]		V <sub>max</sub> , cm <sup>-1</sup> [ε, 10 <sup>4</sup> M <sup>-1</sup> cm <sup>-1</sup> ]		V <sub>max</sub> , cm <sup>-1</sup> [ε, 10 <sup>4</sup> M <sup>-1</sup> cm <sup>-1</sup> ]	
 <b>3</b>	19600 [2.4], 32000 [4.4]		9150 [4.4], 10700 [1.8], 23450 [4.8]		13250 [1.8], 17500 [4.0], 26800 [2.0], 36300 [5.8]	
 <b>7</b>	20200 [4.6], 28600 [4.0]		9350 [2.2], 14850 [0.4], 22250 [2.8], 27250 [3.4], 37698 [5.6]		-	
 <b>8</b>	20550 [2.1], 27550 [4.0] 31 750 [4.1]		8800 [3.0], 23600 [4.5], 30500 [2.9]		8200 [0.4], 10450 [1.5], 17850 [2.6], 26100 [3.3], 36300 [5.6]	
 <b>11</b>	20200 [2.0], 38750 [6.0]		11550 [0.8], 16250 [0.2], 25000 [1.0], 29600 [1.4]		-	
 <b>12</b>	20900 [2.2], 28500 [3.0]		11300 [1.8], 15600 [0.4], 22550 [2.8], 28250 [2.6] 36550 [5.8]		-	
 <b>13</b>	22900 [2.0], 27250 [4.0]		8050 [0.2], 11000 [1.2], 15250 [0.2], 20850 [1.6], 27600 [3.8], 36600 [4.4]		-	
 <b>14</b> <sup>[b]</sup>	31350 [2.3], 38500 [5.0]		12050 [1.0], 17000 [0.1], 27300 [0.7], 29850 [1.3], 35700 [5.2], 36500 [5.3], 37150 [5.4]		-	
 <b>15</b> <sup>[b]</sup>	25750 [3.6], 37900 [sh, 4.5], 40150 [5.0]		11150 [2.0], 15550 [0.5], 22200 [2.6], 24050 [1.8], 35600 [5.4], 36650 [5.5], 37150 [5.3]		-	
 <b>17</b>	20350 [2.4], 26300 [3.6]		9300 [2.0], 14700 [0.6], 21800 [2.6], 33200 [3.8], 37700 [5.0]		-	

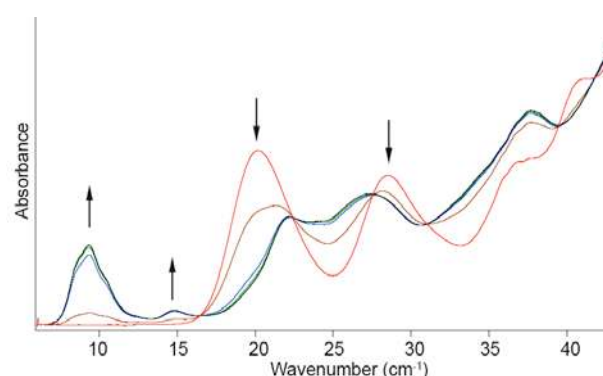
<sup>[a]</sup> Data collected between -15 and -30 °C in CH<sub>2</sub>Cl<sub>2</sub> using an OTTE cell containing Pt grid working, Pt auxiliary and Ag/AgCl reference electrodes.

<sup>[b]</sup> Ref. [25a].

**Hyper-Rayleigh scattering studies.** The quadratic nonlinearities of 1–18 were determined at 1064 nm using the hyper-Rayleigh scattering technique; the results are presented in Table 1, together with the two-level corrected values. We have discussed shortcomings with the two-level model in previous reports; although it is not generally considered adequate for donor-bridge-acceptor organometallic complexes such as those in the present study, it may have some utility in cases where the structural variation is restricted to the molecular components responsible for the low-energy charge transfer bands in the linear optical spectrum.<sup>[14],17]</sup> The hyperpolarizability data were confirmed to be free of multi-photon-induced fluorescence.

Several observations can be made from considering this data. Increasing the length of the non-nitro-functionalized alkynyl ligand in chloro complexes (proceeding from **14** to **15** and then to **1**) results in an increase in  $\beta$  and  $\beta_0$  values. In contrast, increasing the length of the non-nitro-functionalized alkynyl ligand in complexes also bearing a nitro-functionalized alkynyl ligand (proceeding from **16** to **17** and then **2**, **4** to **5**, and **9** to **10**) does not lead to a change in  $\beta$  or  $\beta_0$  within the error margins. Increasing the length of the nitro-functionalized alkynyl ligand (proceeding

from **16** to **4** and then to **9**, **18** to **7**, **3** to **8**, and **17** to **5** and then **10**) results in an increase in  $\beta$  on proceeding from the mono(phenyleneethynylene) **16**, **18**, **3**, and **17** to the



**Figure 9.** UV/Vis/NIR progression observed on application of a 0.8 V potential to a dichloromethane solution of **7**.

## FULL PAPER

di(phenyleneethynylene) examples **4**, **7**, **8**, and **5**, respectively, but this is followed by a decrease in  $\beta$  on proceeding further to the tri(phenyleneethynylene) examples **9** and **10**. Replacing nitro by diethylamino to afford strongly dipolar complexes (proceeding from **18** to **3** and **7** to **8**) results in an increase in  $\beta$  (and for the latter in  $\beta_0$ ), as expected. Surprisingly, the  $\beta$  and  $\beta_0$  values for **18** are significant, despite its pseudo-centrosymmetric structure. Finally, the isomers **4** and **17** and the isomers **9**, **5** and **2** suggest that the optimum location of the ligated ruthenium unit in these short OPEs is a di(phenyleneethynylene) unit removed from the peripheral nitro group.

**Z-scan studies.** The cubic optical nonlinearities of **1-17** were assessed using the Z-scan technique<sup>[26]</sup> with low repetition rate femtosecond pulses over a broad spectral range (from 600-650 to 1500-1650 nm, depending on material absorbance at the short wavelength end and observable NLO activity at the long wavelength end). Closed- and open-aperture experiments were undertaken, affording simultaneous evaluation of the spectral dependencies of the absorptive and refractive components of the hyperpolarizability. The maximal values of the two-photon absorption cross-section  $\sigma_2$ , the real component of the cubic nonlinearity  $\gamma_{\text{real}}$ , and the imaginary component of the cubic nonlinearity  $\gamma_{\text{imag}}$  for the complexes are collected in Table 5; the experimental spectral dependence data are presented in Figures S12-S45. We examined the intensity dependence of the open-aperture Z-scan traces at longer wavelengths and confirmed that, where measurable nPA (n-photon absorption) activity exists, it is 2PA in nature, in contrast to the 3PA and 4PA exhibited by the aforementioned stars and dendrimers.<sup>[10,13,14b]</sup>

As anticipated, the maximal cubic NLO values of these small dipolar complexes are low compared to those of larger ruthenium alkynyl dendrimer<sup>[13,14b]</sup> and star complexes,<sup>[13]</sup> and the data are hampered by large error margins. As we have observed with other ruthenium alkynyl complexes, the  $\gamma_{\text{real}}$  values are negative over most of the spectral range surveyed, with maximal values of  $\gamma_{\text{real}}$  in many cases at similar wavelengths to those of the positive maximal values of  $\gamma_{\text{imag}}$ , and therefore consistent with the expected dependence of  $\gamma_{\text{real}}$  on all nonlinear absorption processes through a nonlinear Kramers-Kronig relationship.<sup>[26]</sup>

Despite the low nonlinearities and large error margins, some tentative structure-property correlations can be made for the 2PA data. Increasing the length of the non-nitro-functionalized alkynyl ligand in chloro complexes (proceeding from **14** to **15** and then to **1**) results in a red-shift of the wavelength of the maximal 2PA data and an increase in the corresponding 2PA cross-section. Increasing the length of the non-nitro-functionalized alkynyl ligand in complexes also bearing a nitro-functionalized alkynyl ligand is less clear; proceeding from **16** to **17** and then **2** red-shifts  $\sigma_{2,\lambda_{\text{max}}}$  and increases  $\sigma_{2,\text{max}}$ , but proceeding from **4** to **5** and **9** to **10** results in a marginal decrease in  $\sigma_{2,\text{max}}$  (the data are equivalent within the error margins). Increasing the length of the nitro-functionalized alkynyl ligand (proceeding from **16** to **4** and then to **9**, **3** to **8**, and **17** to **5** and then **10**) results in an increase in  $\sigma_{2,\text{max}}$  on proceeding from the mono(phenyleneethynylene) **16**, **3**, and **17** to the di(phenyleneethynylene) examples **4**, **8**, and **5**, respectively, but this is followed by a decrease in  $\sigma_{2,\text{max}}$  on proceeding further to the tri(phenyleneethynylene) examples **9** and **10**, mirroring observations with quadratic nonlinearity. Replacing nitro by diethylamino to afford a strongly dipolar

**Table 6.** Linear optical and cubic nonlinear optical data.<sup>a</sup>

Complex	$\lambda_{\text{max}}^b$ [ε] <sup>c</sup>	$\sigma_{2,\lambda_{\text{max}}}^d$ [σ <sub>2</sub> ] <sup>e</sup>	$\gamma_{\text{real}}^f$	$\gamma_{\text{imag}}^g$
<b>14</b>	320 [1.9]	650 [300 ± 100]	-60 ± 20	8 ± 3
<b>15</b>	386 [3.1]	800 [1200 ± 200]	-50 ± 5	50 ± 5
<b>1</b>	413 [3.5]	860 [2100 ± 750]	-250 ± 60	100 ± 35
<b>11</b>	482 [1.6]	900 [250 ± 50]	-140 ± 15	12 ± 3
<b>16</b>	485 [1.6]	880 [550 ± 100]	3 ± 8	25 ± 6
<b>3</b>	499 [1.5]	880 [1500 ± 300]	-300 ± 25 <sup>h</sup>	70 ± 15
<b>17</b>	483 [2.5]	950 [850 ± 250]	-100 ± 30	50 ± 15
<b>2</b>	464 [2.4]	950 [1100 ± 150]	-60 ± 8	70 ± 10
<b>12</b>	471 [2.4]	900 [2300 ± 350]	-150 ± 20	120 ± 20
<b>4</b>	467 [2.7]	1050 [3000 ± 450]	-40 ± 15	220 ± 35
<b>7</b>	481 [3.4]	950 [2100 ± 550]	-300 ± 50	120 ± 30
<b>8</b>	477 [1.3]	1100 [1400 ± 350]	-200 ± 30	110 ± 30
<b>5</b>	472 [2.8]	950 [2200 ± 700]	-250 ± 50	110 ± 30
<b>6</b>	477 [2.8]	950 [1800 ± 500]	-300 ± 40	100 ± 30
<b>13</b>	374 [2.1]	900 [1100 ± 150]	-35 ± 20	55 ± 9
<b>9</b>	380 [3.9]	950 [1700 ± 500]	-190 ± 20	95 ± 30
<b>10</b>	389 [6.9]	950 [1300 ± 450]	-150 ± 10	75 ± 25

<sup>a</sup> CH<sub>2</sub>Cl<sub>2</sub> solvent. <sup>b</sup>  $\lambda_{\text{max}}$  in nm. <sup>c</sup>  $\epsilon$  in 10<sup>4</sup> M<sup>-1</sup> cm<sup>-1</sup>. <sup>d</sup>  $\sigma_{2,\lambda_{\text{max}}}$  in nm. <sup>e</sup>  $\sigma_2$  in GM = 10<sup>-50</sup> cm<sup>4</sup> s. <sup>f</sup>  $\gamma_{\text{real}}$  in 10<sup>-34</sup> esu; data at  $\sigma_{2,\lambda_{\text{max}}}$  wavelength unless specified otherwise. <sup>g</sup>  $\gamma_{\text{imag}}$  in 10<sup>-34</sup> esu; data at  $\sigma_{2,\lambda_{\text{max}}}$  wavelength unless specified otherwise. <sup>h</sup> Data at 900 nm.

complex (proceeding from **7** to **8**) results in a decrease in  $\sigma_{2,\text{max}}$ . Finally, and again mirroring observations with quadratic nonlinearity, the data for the isomers **4** and **17** and the isomers **9**, **5** and **2** suggest that the optimum location of the ligated ruthenium unit to maximize  $\sigma_{2,\text{max}}$  in these short OPEs is a di(phenyleneethynylene) unit removed from the peripheral nitro group.

## Conclusions

The present studies have afforded a range of systematically varied oligo(*p*-phenyleneethynylene)s (OPEs) end-functionalized by a nitro acceptor group and with a bis(dppe)-ligated ruthenium unit at varying locations in the OPE chain. The systematically-varied nature of this series of complexes has enabled a number of molecular structure – electronic/optical property observations to be made.

The possibility of tuning the electron richness of the metal center by alkynyl ligand modification was assessed by measuring the corresponding oxidation potentials using cyclic voltammetry.

## FULL PAPER

Proceeding from chloro to phenylethynyl and then amino-functionalized phenylalkynyl ligand leads to a decrease in the Ru<sup>III</sup> oxidation potential. The same outcome is observed on extending the length of the nitro-functionalized alkynyl ligand from mono- to bis-phenyleneethynylene-containing bridge, but lengthening to a tri(phenyleneethynylene) bridge results in negligible further change; for the latter, the nitro group is sufficiently remote as to no longer affect the metal-centered oxidation potential.

The linear optical properties were examined both experimentally (by UV/Vis/NIR spectroscopy) and theoretically (by TD-DFT studies).  $\pi$ -Bridge lengthening of the nitro-functionalized alkynyl ligand by adding phenyleneethynylene units results in a blue shift in absorption maximum. A two-dimensional potential energy scan on one example and TD-DFT studies on a few selected points on the resultant PE surface suggest that the barriers to rotation of the nitro-functionalized phenylene group (with respect to the metal center) as well as that of the non-functionalized phenyl (with respect to the nitro-functionalized phenylene) are very small, and that a wide range of conformations are in equilibrium with coplanar structures under experimental conditions. The low-energy UV/Vis/NIR data are sensitive to orientation of the aryl groups, the oscillator strength of the higher-energy transition increasing with respect to its lower-energy neighbour, the HOMO  $\rightarrow$  LUMO transition, upon twisting the arylalkynyl ligands out of coplanarity, leading to an apparent blue-shift in the convoluted lowest-energy bands of the twisted forms.

UV/Vis/NIR spectroelectrochemical studies revealed that replacing the chloro ligand with an alkynyl ligand and lengthening the nitro-containing alkynyl ligand both lead to a red shift in the low-energy band in the oxidized form; although we did not undertake calculations on the oxidized forms of the complexes in the present study, calculations of the resting and oxidized states of ruthenium alkynyl complexes lacking nitro substituents and displaying similar trends in experimental data were consistent with a similar decreasing energy of the low-energy LMCT transition.<sup>[17k]</sup> IR spectroelectrochemical studies revealed that the  $\nu(\text{MC}\equiv\text{C})$  band in the IR region of the oxidized forms reduces in energy on  $\pi$ -system lengthening, consistent with increasing contribution of a metallabutatrienylic Ru=C=C=C form.

Trends in quadratic nonlinear optical properties at 1064 nm were also explored. For the mono(alkynyl) complexes, an increase in  $\beta$  and  $\beta_0$  coefficients is observed on progression from phenylethynyl ligand (**14**) through to 4-{4-(phenylethynyl)phenylethynyl}phenylethynyl ligand (**1**), analogous to the trend seen with  $\pi$ -system lengthening in other mono(alkynyl) complexes,<sup>[14d,17f]</sup> and consistent with expectations for complexes with dominant low-energy charge-transfer transitions.

For  $\pi$ -system lengthening at the bis(alkynyl) complexes, increasing the length of the non-nitro-functionalized alkynyl ligand in complexes also bearing a nitro-functionalized alkynyl ligand does not lead to a change in  $\beta$  or  $\beta_0$  within the error margins. However, increasing the length of the nitro-functionalized alkynyl ligand results in an increase in  $\beta$  on proceeding from the mono(phenyleneethynylene) to the di(phenyleneethynylene) examples, but a decrease in  $\beta$  on proceeding to the tri(phenyleneethynylene) examples. The trends in second-order NLO properties for these bis(alkynyl) complexes can be

qualitatively explained if we consider the molecular origin of the hyperpolarizability. As discussed above, the linear absorption spectra are dominated by two distinct MLCT bands: the HOMO  $\rightarrow$  LUMO and HOMO  $\rightarrow$  LUMO+1, corresponding broadly to charge transfer to the nitro-functionalized alkynyl ligand and charge transfer to the alkynyl ligand lacking a nitro group, respectively (this generalization weakens on  $\pi$ -system lengthening as the HOMO takes on greater alkynyl ligand character and the LUMO+1 becomes increasingly diffuse, but we believe that this broad argument has validity). If we assume that these two electronic transitions dominate the quadratic nonlinearities  $\beta$  (truncating the sum-over-excited-states summation as below: for clarity, we have omitted the subscript zzz), and we also neglect the three-state contributions  $\beta_{12}$  and  $\beta_{21}$  (because the overlap of the LUMOs and LUMO+1s are small and so the transition dipole moments will be (near) zero), we can simplify the summations to:

$$\beta \approx \beta_1 + \beta_2 + \beta_{12} + \beta_{21} \approx \beta_1 + \beta_2$$

in which  $\beta_1$  is correlated with the HOMO  $\rightarrow$  LUMO transition ( $\lambda_{\text{max},1}$ ) and  $\beta_2$  is correlated with the HOMO  $\rightarrow$  LUMO+1 transition ( $\lambda_{\text{max},2}$ ). A qualitative analysis suggests that the  $\Delta\mu_{\text{eg}}$  values (the differences between the excited-state and ground-state dipole moments) that are derived from the lower-energy MLCT and the higher-energy MLCT transitions have opposite signs. At long wavelengths (ca. > 960 nm), the sign of  $\beta_1$  will be opposite to that of  $\beta_2$ , and consequently a (partial) cancellation occurs. Note that the wavelength where all measurements were conducted (1064 nm) lies in this range, and the unexpectedly low HRS signals for these bis(alkynyl) complexes compared to those seen for nitro-functionalized mono(alkynyl) complexes<sup>[7,14d,17f]</sup> can be directly correlated to this. Interestingly, this model suggests that  $\beta$  is strongly resonance-enhanced between the two-photon resonance frequencies of the MLCT transitions (ca. 720-960 nm, i.e. the region between  $2\lambda_{\text{max},2}$  and  $2\lambda_{\text{max},1}$ ). An oscillatory behaviour is anticipated at wavelengths less than 720 nm (i.e. shorter than  $2\lambda_{\text{max},2}$ ); it is, therefore, difficult to predict  $\beta$  qualitatively in this region because of its dependence upon the relative magnitudes of  $\beta_1$  and  $\beta_2$ , but it is expected that  $\beta$  will be lower than the maximal value in the region between  $2\lambda_{\text{max},2}$  and  $2\lambda_{\text{max},1}$ , due to the increasing denominator  $D_{p,q}$  at shorter wavelengths (higher energy). The decrease in  $\beta$  seen on proceeding from **4** to **9** and **5** to **10** can be attributed to the simultaneous blue shift in the lowest-energy absorption band (**4**: 472 nm, **5**: 470 nm cf. **9**: 435 nm, **10**: 433 nm) while the position of the higher-energy MLCT band is approximately the same (ca. 380 nm) for **4**, **5**, **9**, and **10**. The smaller energy separation of  $\lambda_{\text{max},1}$  and  $\lambda_{\text{max},2}$  in **9** and **10** results in a more pronounced cancellation of  $\beta_1$  and  $\beta_2$  in the long-wavelength region where the measurements were undertaken: the  $\beta_1$  maximum is blue shifted, and its proximity to the maximum of  $\beta_2$  results in the maximal value of  $\beta$  decreasing accordingly. This model explains the unexpected decrease in the HRS signal upon elongation of the conjugated system, compared to the monotonically increasing  $\beta$  value observed for the (mono)alkynyl complexes.

Complexes possessing the same number of PE groups at each alkynyl ligand, but with different functionalization of these ligands, have also been explored. Interestingly, the complexes *trans*-[Ru{(C $\equiv$ C-1,4-C<sub>6</sub>H<sub>4</sub>)<sub>n</sub>NO<sub>2</sub>}(C $\equiv$ CR)(dppe)<sub>2</sub>] (n = 1, R = 1,4-C<sub>6</sub>H<sub>4</sub>NEt<sub>2</sub> (**3**), Ph (**16**), 1,4-C<sub>6</sub>H<sub>4</sub>NO<sub>2</sub> (**18**)) exhibit similar

## FULL PAPER

experimental and two-level corrected quadratic nonlinearities (and the data for **18** are not zero/close to zero, as may have been anticipated for an apparently centrosymmetric molecule). We believe that the low barrier to rotation of the phenylalkynyl ligands results in contributions from (pseudo)  $D_2$  octupolar symmetry (and thereby non-centrosymmetric) structures in which the planes of the alkynyl ligand aryl groups proximal to the metal center are orthogonal; similar observations with porphyrin-based assemblies are extant.<sup>[27]</sup> The three complexes are not optically transparent at the second-harmonic wavelength (532 nm: see Figure 5). Complex **3**, in particular, exhibits an optical absorption maximum very close to that wavelength and its calculated  $\beta_0$  value may be an over-correction.

We have also identified structure-property trends from the 2PA data, while being mindful of (in many cases) the large error margins. Similar outcomes to those from the aforementioned HRS studies were noted: increasing the length of the non-nitro-functionalized alkynyl ligand in chloro complexes results in an increase in 2PA cross-section, while increasing the length of the non-nitro-functionalized alkynyl ligand in complexes also bearing a nitro-functionalized alkynyl ligand is less clear. Increasing the length of the nitro-functionalized alkynyl ligand results in an increase in  $\sigma_{2,\max}$  on proceeding from mono- to diphenyleneethynylene, but this is followed by a decrease in  $\sigma_{2,\max}$  on proceeding further to tri-phenyleneethynylene bridge. Finally, the data for positional isomers were examined, the results suggesting that  $\sigma_{2,\max}$  is maximized when the metal center is a di(phenyleneethynylene) unit from the peripheral nitro group.

## Acknowledgements

We thank the Australian Research Council, the Fund for Scientific Research-Flanders (FWO-Vlaanderen; FWO G.0312.08) and the Katholieke Universiteit Leuven (GOA/2006/03) for financial support, and Yuwen Wu (ANU) for providing a crystal of **14** suitable for the X-ray diffraction study.

**Keywords:** HRS • ruthenium • alkynyl • TD-DFT • spectroelectrochemistry

## References

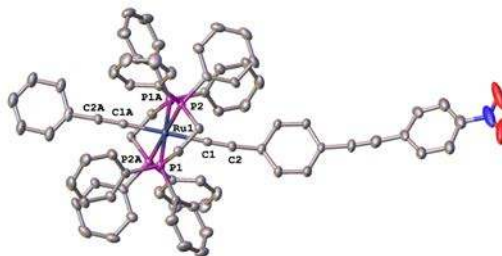
- [1] a) B. J. Coe, in *Comprehensive Coordination Chemistry II*, Vol. 9 (Eds.: J. A. McCleverty, T. J. Meyer.), Elsevier, Oxford, UK, **2004**, pp. 621-687; b) M. E. Thompson, P. E. Djurovich, S. Barlow, S. Marder, in *Comprehensive Organometallic Chemistry III*, Vol. 12 (Eds.: R. H. Crabtree, D. M. P. Mingos), Elsevier, Oxford, **2007**, pp. 101-194; c) J. P. L. Morrall, G. T. Dalton, M. G. Humphrey, M. Samoc, *Adv. Organomet. Chem.* **2007**, *55*, 61-136; d) C. Andraud, O. Maury, *Eur. J. Inorg. Chem.* **2009**, 4357-4371; e) K. A. Green, M. P. Cifuentes, M. Samoc, M. G. Humphrey, *Coord. Chem. Rev.* **2011**, *255*, 2025-2038; f) M. G. Humphrey, T. Schwich, P. J. West, M. P. Cifuentes, M. Samoc, in *Comprehensive Inorg. Chem. II* (Eds.: J. Reedijk, K. Poeppelmeier), Elsevier, Oxford, UK, **2013**, pp. 781-835.
- [2] See, for example: a) D. J. Williams, *Nonlinear Optical Properties of Organic and Polymeric Materials*, ACS Symposium Series, Vol. 233, American Chemical Society, Washington, D.C., **1983**; b) D. S. Chemla, J. Zyss, *Nonlinear Optical Properties of Organic Molecules and Crystals I*, Academic Press, Orlando, **1987**; c) D. S. Chemla, J. Zyss, *Nonlinear Optical Properties of Organic Molecules and Crystals II*, Academic Press, Orlando, **1987**; d) *Nonlinear Optical Properties of Polymers*, (Eds.: A. J. Heeger, J. Orenstein, D. R. Ulrich), Materials Research Society, Pittsburgh, **1988**; e) R. A. Hann, D. Bloor, *Organic Materials for Nonlinear Optics*, Royal Society of Chemistry, London, **1989**; f) *Materials for Non-linear and Electro-optics*, (Ed.: M. H. Lyons), Institute of Physics, Bristol, **1989**; g) S. R. Marder, J. W. Perry, W. P. Schaefer, E. J. Ginsburg, C. B. Gorman, R. H. Grubbs, *Mat. Res. Soc. Symp. Proc.* **1990**, *175*, 101-106.
- [3] a) B. J. Coe, S. Houbrechts, I. Asselberghs, A. Persoons, *Angew. Chem., Int. Ed.* **1999**, *38*, 366-369; b) T. Weyland, I. Ledoux, S. Brasselet, J. Zyss, C. Lapinte, *Organometallics* **2000**, *19*, 5235-5237; c) M. Malaun, Z. R. Reeves, R. L. Paul, J. C. Jeffery, J. A. McCleverty, M. D. Ward, I. Asselberghs, K. Clays, A. Persoons, *Chem. Commun.* **2001**, 49; d) F. Paul, K. Costuas, I. Ledoux, S. Deveau, J. Zyss, J.-F. Halet, C. Lapinte, *Organometallics* **2002**, *21*, 5229; e) B. J. Coe, N. R. M. Curati, *Comments Inorg. Chem.* **2004**, *25*, 147-184; f) I. Asselberghs, K. Clays, A. Persoons, A. M. McDonagh, M. D. Ward, J. McCleverty, *Chem. Phys. Lett.* **2003**, *368*, 408-411.
- [4] See, for example: a) M. L. H. Green, S. R. Marder, M. E. Thompson, J. A. Bandy, D. Bloor, P. V. Kolinsky, R. J. Jones, *Nature* **1987**, *330*, 360-362; b) Y. Shi, C. Zhang, J. H. Bechtel, L. R. Dalton, B. H. Robinson, W. H. Steier, *Science* **2000**, *288*, 119-122; c) W. Wenseleers, E. Goovaerts, P. Hepp, M. H. Garcia, M. P. Robalo, A. R. Dias, M. F. M. Piedade, M. T. Duarte, *Chem. Phys. Lett.* **2003**, *367*, 390-397; d) S. Lui, M. A. Haller, H. Ma, L. R. Dalton, S.-H. Jang, A. K.-Y. Jen, *Adv. Mater.* **2003**, *127*, 2758-2760; e) Y. Liao, B. E. Eichinger, K. A. Firestone, M. Haller, J. D. Luo, W. Kaminsky, J. B. Benedict, P. J. Reid, A. K. Y. Jen, L. R. Dalton, B. H. Robinson, *J. Am. Chem. Soc.* **2005**, *127*, 2758-2766; f) M. Fuentealba, L. Toupet, C. Manzur, D. Carrillo, I. Ledoux-Rak, J. R. Hamon, *J. Organomet. Chem.* **2007**, *692*, 1099-1109; g) S. Steffens, M. H. Prosenec, J. Heck, I. Asselberghs, K. Clays, *Eur. J. Inorg. Chem.* **2008**, 1999-2006.
- [5] a) C. E. Powell, M. G. Humphrey, *Coord. Chem. Rev.* **2004**, *248*, 725-756; b) G. Grelaud, M. P. Cifuentes, F. Paul, M. G. Humphrey, *J. Organomet. Chem.* **2014**, *751*, 181-200.
- [6] S. R. Marder, D. N. Beratan, B. G. Tiemann, L. T. Cheng, W. Tam, *Organic Materials for Nonlinear Optics II*, (Eds.: R. A. Hann, D. Bloor), Royal Society of Chemistry: London, **1991**, p. 165.
- [7] J. P. Morrall, M. P. Cifuentes, M. G. Humphrey, R. Kellens, E. Robijns, I. Asselbergh, K. Clays, A. Persoons, M. Samoc, A. C. Willis, *Inorg. Chim. Acta* **2006**, *359*, 998-1005.
- [8] J. L. Oudar, D. S. Chemla, *J. Chem. Phys.* **1977**, *66*, 2664-2668.
- [9] G. T. Dalton, M. P. Cifuentes, S. Petrie, R. Stranger, M. G. Humphrey, M. Samoc, *J. Am. Chem. Soc.* **2007**, *129*, 11882-11883.
- [10] T. Schwich, A. Barlow, M. P. Cifuentes, J. Szeremeta, M. Samoc, M. G. Humphrey, *Chem. Eur. J.* **2017**, *23*, 8395-8399.
- [11] a) M. Samoc, G. T. Dalton, J. A. Gladysz, Q. Zheng, Y. Velkov, H. Ågren, P. Norman, M. G. Humphrey, *Inorg. Chem.* **2008**, *47*, 9946-9957; b) G. T. Dalton, M. P. Cifuentes, L. A. Watson, S. Petrie, R. Stranger, M. Samoc, M. G. Humphrey, *Inorg. Chem.* **2009**, *48*, 6534-6547; c) B. Gao, L. M. Mazur, M. Morshedi, A. Barlow, H. Wang, C. Quintana, C. Zhang, M. Samoc, M. P. Cifuentes, M. G. Humphrey, *Chem. Commun.* **2016**, 8301-8304.
- [12] a) R. L. Roberts, T. Schwich, T. C. Corkery, M. P. Cifuentes, K. A. Green, J. D. Farmer, P. J. Low, T. B. Marder, M. Samoc, M. G. Humphrey, *Adv. Mater.* **2009**, *21*, 2318-2322; b) T. Schwich, M. P. Cifuentes, P. A. Gugger, M. Samoc, M. G. Humphrey, *Adv. Mater.* **2011**, *23*, 1433-1435.
- [13] P. V. Simpson, L. A. Watson, A. Barlow, G. Wang, M. P. Cifuentes, M. G. Humphrey, *Angew. Chem. Int. Ed.* **2016**, *55*, 2387-2391.
- [14] a) C. E. Powell, J. P. L. Morrall, S. A. Ward, M. P. Cifuentes, E. G. A. Notaras, M. Samoc, M. G. Humphrey, *J. Am. Chem. Soc.* **2004**, *126*, 12234-12235; b) M. Samoc, J. P. Morrall, G. T. Dalton, M. P. Cifuentes, M. G. Humphrey, *Angew. Chem. Int. Ed.* **2007**, *46*, 73-733; c) C. E. Powell, S. Hurst, J. P. Morrall, M. P. Cifuentes, R. L. Roberts, M. Samoc, M. G. Humphrey, *Organometallics* **2007**, *26*, 4456-4463; d) B. A. Babgi, L. Rigamonti, M. P. Cifuentes, T. C. Corkery, M. D. Randles, T. Schwich, S. Petrie, R. Stranger, A. Teshome, I. Asselberghs, K. Clays, M. Samoc, M. G. Humphrey, *J. Am. Chem. Soc.* **2009**, *131*, 10293-10307; e) K. A. Green, M. P. Cifuentes, T. C. Corkery, M. Samoc, M. G. Humphrey, *Angew. Chem. Int. Ed.* **2009**, *48*, 7867-7870; f) C. J. Jeffery, M. P. Cifuentes, G. T. Dalton, T. C. Corkery, M. D. Randles, A. C. Willis, M. Samoc, M. G. Humphrey,

- Macromol. Rapid Commun.* **2010**, *31*, 846-849; g) M. Samoc, T. C. Corkery, A. M. McDonagh, M. P. Cifuentes, M. G. Humphrey, *Aust. J. Chem.* **2011**, *64*, 1269-1273; h) K. A. Green, P. V. Simpson, T. C. Corkery, M. P. Cifuentes, M. Samoc, M. G. Humphrey, *Macromol. Rapid Commun.* **2012**, *33*, 573-578; i) Z. Chen, C. J. Jeffery, M. Morshedi, G. J. Moxey, A. Barlow, X. Yang, B. A. Babgi, G. T. Dalton, M. D. Randles, M. K. Smith, C. Zhang, M. Samoc, M. P. Cifuentes, M. G. Humphrey, *ChemPlusChem* **2015**, *80*, 1329-1340; j) H. Zhang, M. Morshedi, M. S. Kodikara, G. J. Moxey, G. Wang, H. Wang, C. Quintana, R. Stranger, C. Zhang, M. P. Cifuentes, M. G. Humphrey, *ChemPlusChem* **2016**, *81*, 613-620.
- [15] a) D. Touchard, C. Morice, V. Cadierno, P. Haquette, L. Toupet, P. H. Dixneuf, *J. Chem. Soc., Chem. Commun.* **1994**, 859-860; b) A. M. McDonagh, M. P. Cifuentes, I. R. Whittall, M. G. Humphrey, M. Samoc, B. Luther-Davies, D. C. R. Hockless, *J. Organomet. Chem.* **1996**, *526*, 99-103; c) D. Touchard, P. Haquette, S. Guesmi, L. L. Pichon, A. Daridor, L. Toupet, P. H. Dixneuf, *Organometallics* **1997**, *16*, 3640-3648; d) A. M. McDonagh, C. E. Powell, J. P. Morrall, M. P. Cifuentes, M. G. Humphrey, *Organometallics* **2003**, *22*, 1402-1413; e) S. K. Hurst, N. T. Lucas, M. G. Humphrey, T. Isoshima, K. Wostyn, I. Asselberghs, K. Clays, A. Persoons, M. Samoc, B. Luther-Davies, *Inorg. Chim. Acta* **2003**, *350*, 62-76.
- [16] K. Lau, A. Barlow, G. J. Moxey, Q. Li, Y. Liu, M. G. Humphrey, M. P. Cifuentes, T. Frankcombe, R. Stranger, *Phys. Chem. Chem. Phys.* **2015**, *17*, 10781-10785.
- [17] a) C. Bitcon, M. W. Whiteley, *J. Organomet. Chem.* **1987**, *336*, 385-392; b) I. R. Whittall, M. P. Cifuentes, M. G. Humphrey, B. Luther-Davies, M. Samoc, S. Houbrechts, A. Persoons, G. A. Heath, D. Bogsanyi, *Organometallics* **1997**, *16*, 2631-2637; c) R. H. Naulty, A. M. McDonagh, I. R. Whittall, M. P. Cifuentes, M. G. Humphrey, S. Houbrechts, J. Maes, A. Persoons, G. A. Heath, D. C. R. Hockless, *J. Organomet. Chem.* **1998**, *563*, 137-146; d) A. M. McDonagh, M. P. Cifuentes, M. G. Humphrey, S. Houbrechts, J. Maes, A. Persoons, M. Samoc, B. Luther-Davies, *J. Organomet. Chem.* **2000**, *610*, 71-79; e) E. Stein, S. Y. Oki, E. J. S. Vichi, *J. Braz. Chem. Soc.* **2000**, *11*, 252-256; f) S. Hurst, M. P. Cifuentes, J. P. L. Morrall, N. T. Lucas, I. R. Whittall, M. G. Humphrey, I. Asselberghs, A. Persoons, M. Samoc, B. Luther-Davies, A. C. Willis, *Organometallics* **2001**, *20*, 4664-4675; g) S. K. Hurst, N. T. Lucas, M. G. Humphrey, I. Asselberghs, R. Van Boxel, A. Persoons, *Aust. J. Chem.* **2001**, *54*, 447-451; h) M. P. Cifuentes, C. E. Powell, M. G. Humphrey, G. A. Heath, M. Samoc, B. Luther-Davies, *J. Phys. Chem. A* **2001**, *105*, 9625-9627; i) W.-Y. Wong, C.-K. Wong, G.-L. Lu, *J. Organomet. Chem.* **2003**, *671*, 27-34; j) S. Rigaut, J. Perruchon, L. Le Pichon, D. Touchard, P. H. Dixneuf, *J. Organomet. Chem.* **2003**, *670*, 37-44; k) C. E. Powell, M. P. Cifuentes, J. P. L. Morrall, R. Stranger, M. G. Humphrey, M. Samoc, B. Luther-Davies, G. A. Heath, *J. Am. Chem. Soc.* **2003**, *125*, 602-610; l) C. E. Powell, M. G. Humphrey, M. P. Cifuentes, J. P. Morrall, M. Samoc, B. Luther-Davies, *J. Phys. Chem. A* **2003**, *107*, 11264-11266; m) K. Onitsuka, N. Ohara, F. Takei, S. Takahashi, *Dalton Trans.* **2006**, 3693-3698; n) N. Gauthier, C. Olivier, S. Rigaut, D. Touchard, T. Roisnel, M. G. Humphrey, F. Paul, *Organometallics* **2008**, *27*, 1063-1072; o) F. Meng, Y.-M. Hervault, Q. Shao, B. Hu, L. Norel, S. Rigaut, X. Chen, *Nature Commun.* **2014**, *5*, 3023-1-3023-9; p) H. Zhao, P. V. Simpson, A. Barlow, G. J. Moxey, M. Morshedi, N. Roy, R. Philip, C. Zhang, M. P. Cifuentes, M. G. Humphrey, *Chem. Eur. J.* **2015**, *21*, 11843 - 11854; q) M. C. Walkey, L. T. Byrne, M. J. Piggott, P. J. Low, G. A. Koutsantonis, *Dalton Trans.* **2015**, *44*, 8812-8815.
- [18] M. Younus, N. J. Long, P. R. Raithby, J. Lewis, N. A. Page, A. J. P. White, D. J. Williams, M. C. B. Colbert, A. J. Lodge, M. S. Khan, D. G. Parker, *J. Organomet. Chem.* **1999**, *578*, 198-209.
- [19] L. Rigamonti, B. Babgi, M. P. Cifuentes, R. L. Roberts, S. Petrie, R. Stranger, S. Righetto, A. Teshome, I. Asselberghs, K. Clays, M. G. Humphrey, *Inorg. Chem.* **2009**, *48*, 3562-3572.
- [20] a) M. P. Cifuentes, M. G. Humphrey, M. Samoc, B. Babgi, G. T. Dalton, L. Rigamonti, *Polym. Prepr. (Am. Chem. Soc., Div. Polym. Chem.)* **2009**, *50*, 515; b) H. Sahnoune, N. Gauthier, K. Green, K. Costuas, F. Paul, J. F. Halet, *Aust. J. Chem.* **2015**, *68*, 1352-1358.
- [21] a) M. Biswas, P. Nguyen, T. B. Marder, L. R. J. Khundkar, *J. Phys. Chem. A* **1997**, *101*, 1689-1695; b) P. Nguyen, G. Lesley, T. B. Marder, I. Ledoux, J. Zyss, *J. Chem. Mater.* **1997**, *9*, 406-408; c) A. Beeby, K. Findlay, P. J. Low, T. B. Marder, *J. Am. Chem. Soc.* **2002**, *124*, 8280-8284; d) J. S. Siddle, R. M. Ward, J. C. Collings, S. R. Rutter, L. Porrès, L. Applegarth, A. Beeby, A. S. Batsanov, A. L. Thompson, J. A. K. Howard, A. Boucekkinne, K. Costuas, J.-F. Halet, T. B. Marder, *New J. Chem.* **2007**, *31*, 841-851.
- [22] A. L. Spek, *J. Appl. Cryst.* **2003**, *36*, 7-13.
- [23] T. Yanai, D. P. Tew, N. C. Handy, *Chem. Phys. Lett.* **2004**, *393*, 51-57.
- [24] E. Kulasekera, S. Petrie, R. Stranger, M. G. Humphrey, *Organometallics* **2014**, *33*, 2434-2447.
- [25] a) C. E. Powell, M. P. Cifuentes, J. P. Morrall, R. Stranger, M. G. Humphrey, M. Samoc, B. Luther-Davies, G. A. Heath, *J. Am. Chem. Soc.* **2003**, *125*, 602-610; b) N. Gauthier, N. Tchouar, F. Justaud, G. Argouarch, M. P. Cifuentes, L. Toupet, D. Touchard, J.-F. Halet, S. Rigaut, M. G. Humphrey, K. Costuas, F. Paul, *Organometallics* **2009**, *28*, 2253-2266.
- [26] M. Sheik-Bahae, D. J. Hagan, E. W. van Stryland, *Phys. Rev. Lett.* **1990**, *65*, 96-99.
- [27] T. V. Duncan, K. Song, S.-T. Hung, I. Miloradovic, A. Nayak, A. Persoons, T. Verbiest, M. J. Thérien, K. Clays, *Angew. Chem. Int. Ed.* **2008**, *47*, 2798-2981.

## Entry for the Table of Contents

## FULL PAPER

Quadratic and cubic optical nonlinearities of oligo(*p*-phenyleneethynylene)s (nOPEs) end-functionalized by a nitro acceptor group and with a ligated ruthenium unit at varying locations in the nOPE chain increase on proceeding from 1PE to 2PE, but decrease on further chain lengthening, defining the optimum bridge length for NLO effects in such complexes.



*Bandar A. Babgi, Mahesh S. Kodikara, Mahbod Morshedi, Huan Wang, Cristóbal Quintana, Torsten Schwich, Graeme J. Moxey, Nick van Steerteghem, Koen Clays, Robert Stranger, Marie P. Cifuentes, and Mark G. Humphrey\**

**Page No. – Page No.**

**Linear Optical, Quadratic and Cubic Nonlinear Optical, Electrochemical, and Theoretical Studies of “Rigid-Rod” Bis(Alkynyl)Ruthenium Complexes**